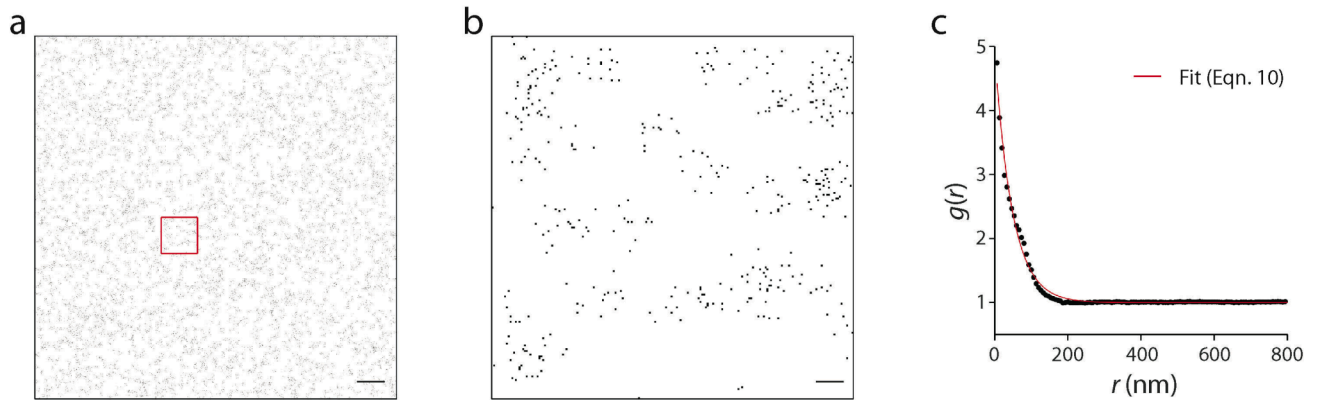


Probing protein heterogeneity in the plasma membrane using PALM and pair correlation analysis

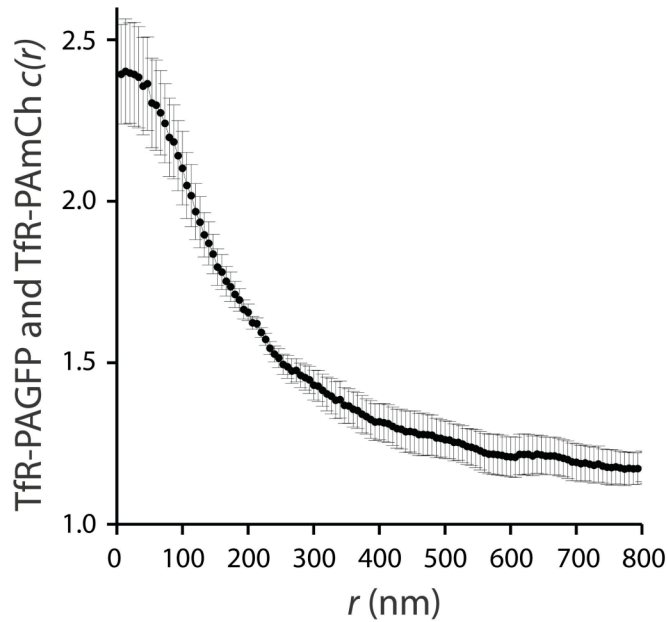
Prabuddha Sengupta, Tijana Jovanovic-Talisman, Dunja Skoko¹, Malte Renz, Sarah L Veatch & Jennifer Lippincott-Schwartz

Supplementary Figure 1	Distribution of simulated clustered molecules and fit of their autocorrelation function to exponential model.
Supplementary Figure 2	Cross-correlation between TfR-PAGFP and TfR-PAmCh transiently expressed in COS-7 cells.
Supplementary Figure 3	Representative fits of measured autocorrelation ($g(r)^{\text{peaks}}$) to clustered model.
Supplementary Figure 4	Proteins per cluster (N^{cluster}) distribution of PAGFP-labeled Lyn and LAT at steady state revealed by PC-PALM.
Supplementary Figure 5	Proteins per cluster (N^{cluster}) distribution of PAGFP-GPI at two different temperatures assessed by PC-PALM.
Supplementary Figure 6	Localization precision of PAGFP-labeled proteins and purified PAGFP
Supplementary Figure 7	Fit of distribution of localization precision of peaks to skewed Gaussian function
Supplementary Note 1	Computation of Correlation Functions
Supplementary Note 2	Definition of Mathematical Terms



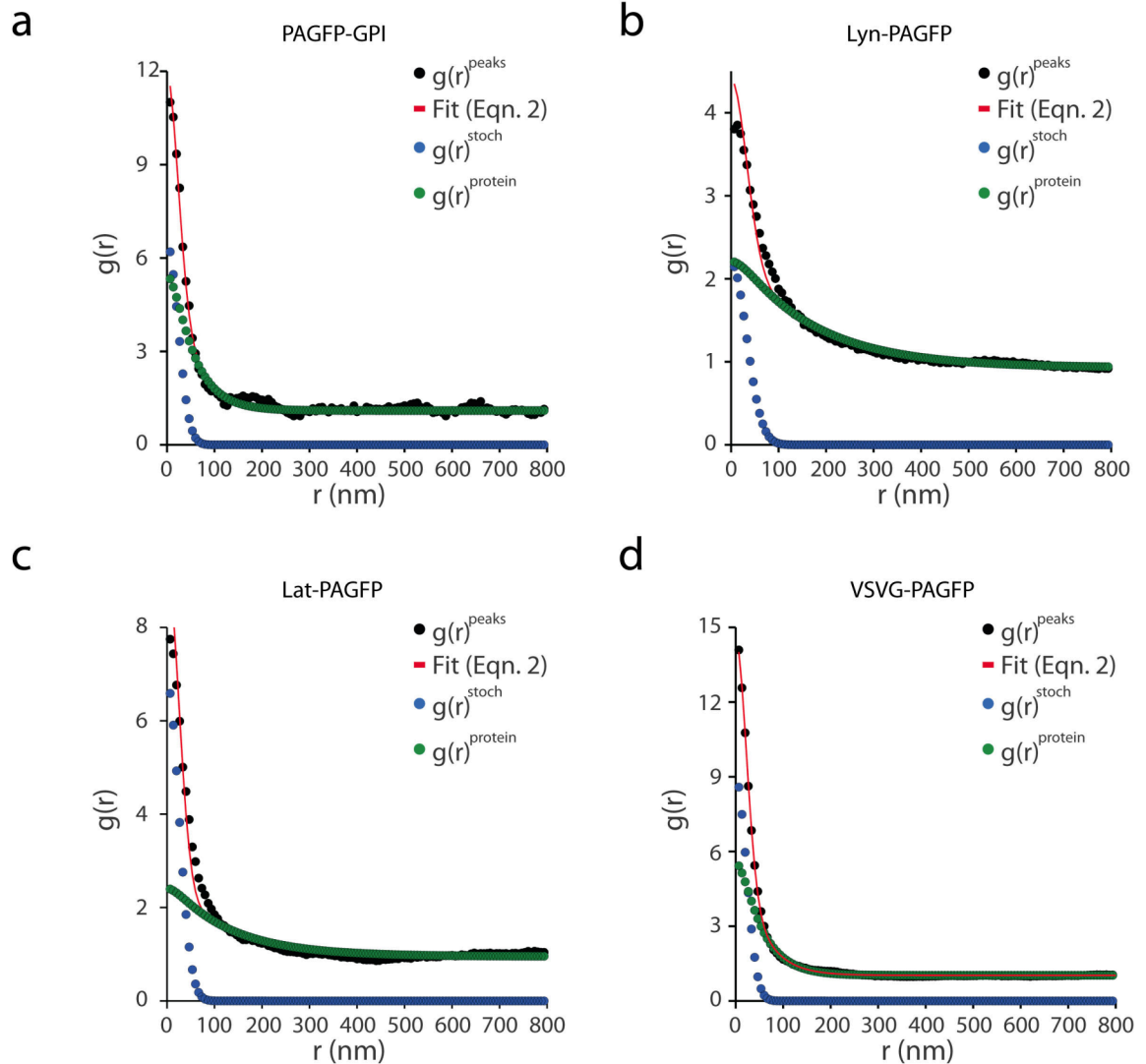
Supplementary Figure 1. Distribution of simulated clustered molecules and fit of their autocorrelation function to exponential model.

Autocorrelation function of simulated clustered molecules distributed over a two dimensional surface can be fit with a model where the correlation of proteins decay as an exponential function (Eqn. 10 in Methods). **(a)** Simulated image of molecules distributed in randomly shaped clusters over an area of $13.3 \times 13.3 \mu\text{m}^2$, and with average number of molecules in a cluster equal to 10; scale bar $1 \mu\text{m}$. **(b)** Zoomed in section of simulated image marked by red box in **(a)**; scale bar 100 nm. **(c)** Fit of Eqn. 10 (red line) to computed autocorrelation function of the simulated image ($R^2 = 0.99$; $\xi = 51 \text{ nm}$; $A = 3.9$, $N^{\text{cluster}} = 10.8$).



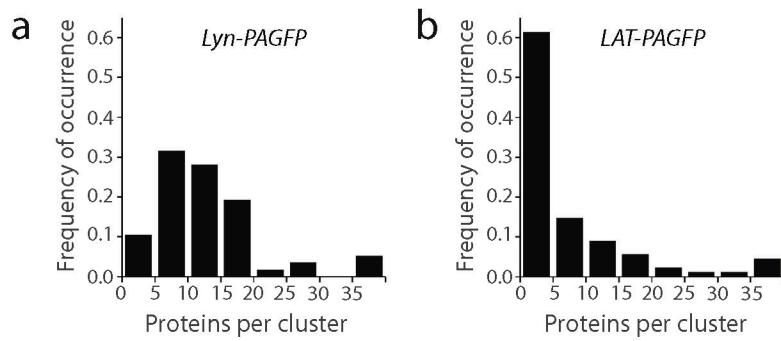
Supplementary Figure 2. Cross-correlation between TfR-PAGFP and TfR-PAmCh transiently expressed in COS-7 cells.

Average cross-correlation from 4 randomly chosen sections of a cell. TfR-PAGFP and TfR-PAmCh show strong spatial correlation as evident from the $c(r)$ value (> 1), indicating that the two molecules co-cluster on the PM.



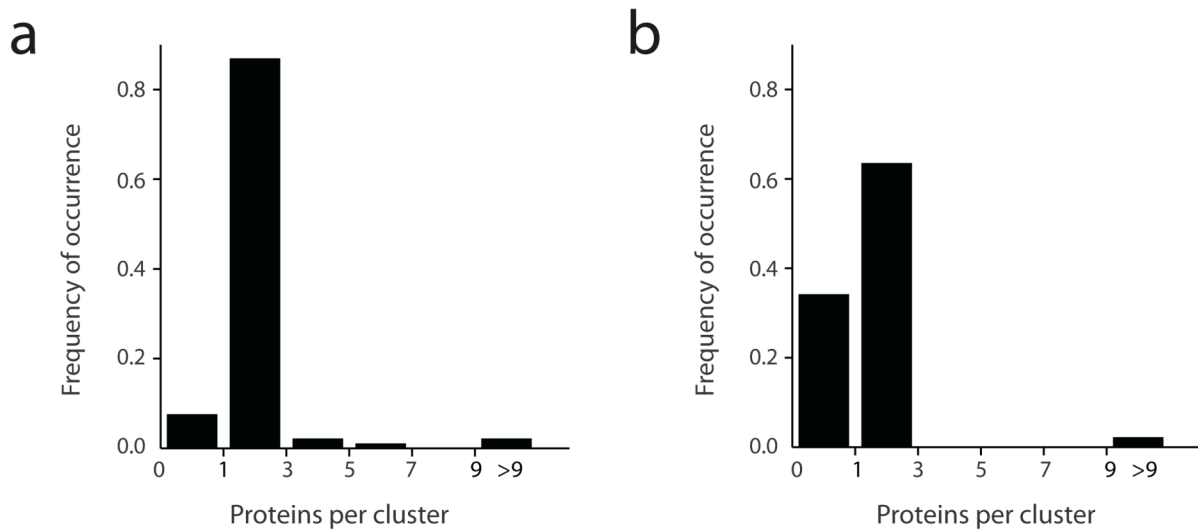
Supplementary Figure 3. Representative fits of measured autocorrelation ($g(r)^{\text{peaks}}$) to clustered model.

Graphs show the fit (red line) of the correlation function of a section of a cell expressing **(a)** PAGFP-GPI ($R^2 = 0.99$; $\zeta = 46$ nm; $A = 6.4$), **(b)** Lyn-PAGFP ($R^2 = 0.98$; $\zeta = 163$ nm; $A = 1.5$), **(c)** Lat-PAGFP ($R^2 = 0.97$; $\zeta = 126$ nm; $A = 1.7$), and, **(d)** VSVG-PAGFP ($R^2 = 0.99$; $\zeta = 46$ nm; $A = 6.6$), respectively, to the clustered model (Eqn. 2 in text, Eqn. 10 in Methods). Correlation due to multiple appearances of a single protein ($g(r)^{\text{stoch}}$) and protein correlation ($g(r)^{\text{protein}}$) were calculated from the fit parameters. Note that PAGFP-GPI and VSVG-PAGFP show fast decaying correlation curve (shorter correlation length), while Lyn-PAGFP and Lat-PAGFP show longer-range correlation. Additionally, GPI and VSVG show significantly higher values of γ -intercept than Lyn and Lat, indicating that GPI and VSVG have higher local density in clusters.



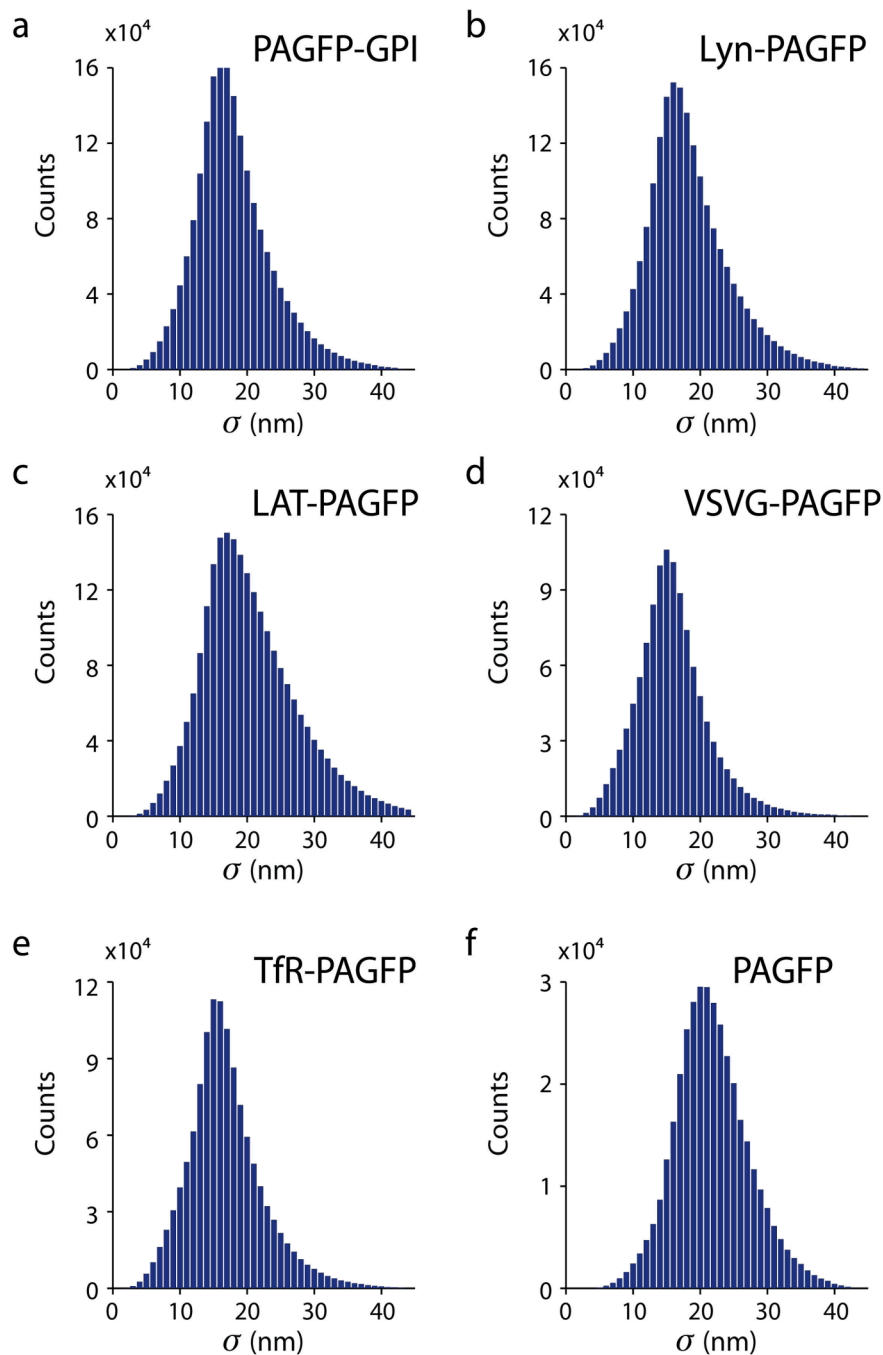
Supplementary Figure 4. Proteins per cluster (N^{cluster}) distribution of PAGFP-labeled Lyn and LAT at steady state revealed by PC-PALM.

(a) Lyn-PAGFP and **(b)** Lat-PAGFP were organized into clusters with variable number of proteins, having up to 40 detectable proteins.



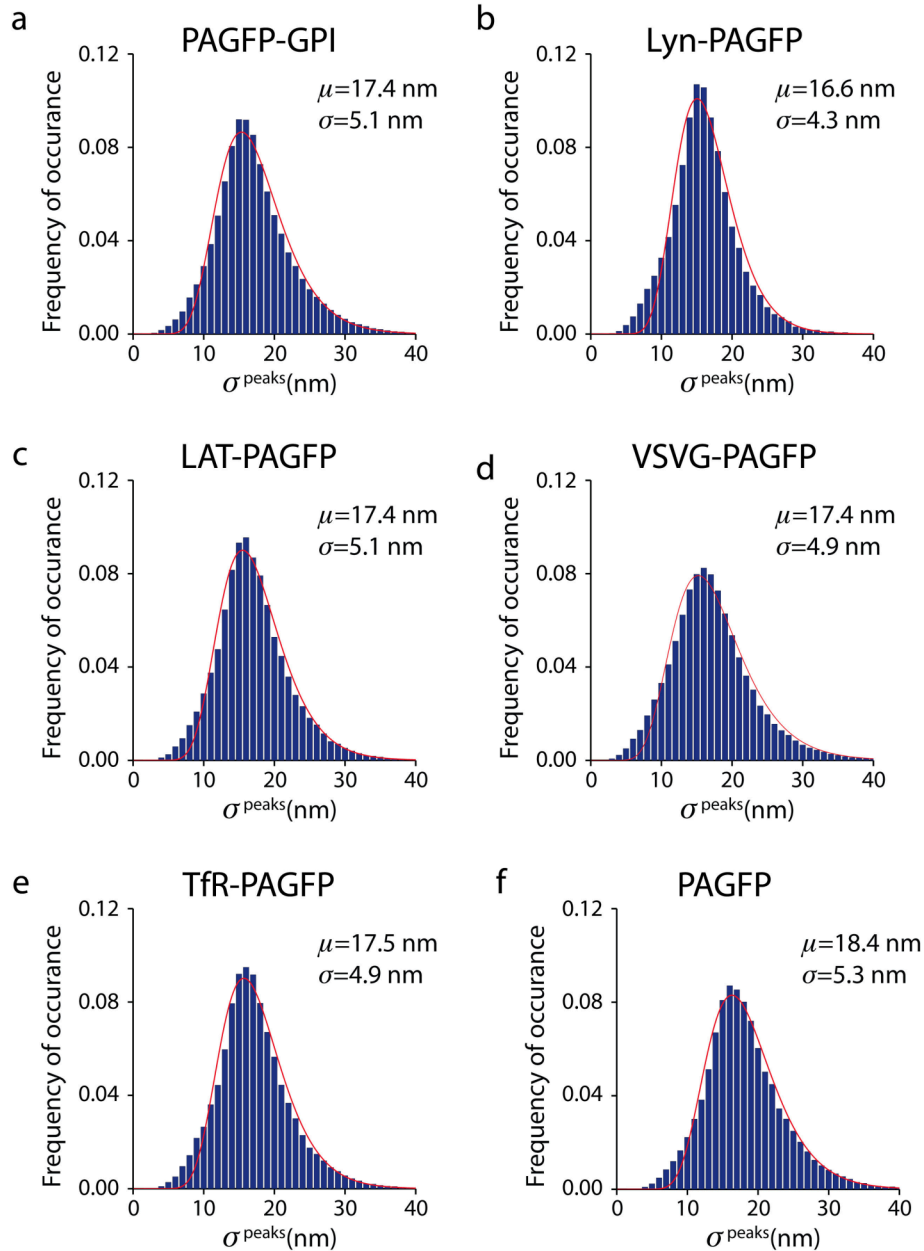
Supplementary Figure 5. Proteins per cluster (N^{cluster}) distribution of PAGFP-GPI at two different temperatures assessed by PC-PALM.

Number of proteins per cluster decreases upon lowering the temperature from 37 °C (**a**) to 4 °C (**b**).



Supplementary Figure 6. Localization precision of PAGFP-labeled proteins and purified PAGFP

(a-e) Localization precision of PAGFP-labeled proteins expressed in COS-7 cells. Distribution of localization precision of peaks (σ^{peaks}) of PAGFP-GPI (mean, 18; median, 17.2), Lyn-PAGFP (mean, 18.2; median, 17.4), Lat-PAGFP (mean, 20.5; median, 19.4), VSVG-PAGFP (mean, 15.9; median, 15.4), and TfR-PAGFP (mean, 16.8; median, 16.2), respectively. **(f)** σ^{peaks} distribution of purified PAGFP molecules covalently immobilized onto coverslips (mean, 21.7; median, 21.3).



Supplementary Figure 7. Fit of distribution of localization precision of peaks to skewed Gaussian function

Fitting of distribution of localization precision of peaks (σ^{peaks}) detected from either cells expressing PAGFP-labeled proteins or PAGFP immobilized on coverslips. **(a-e)** Distribution of σ^{peaks} from a representative cell expressing PAGFP-GPI, Lyn-PAGFP, Lat-PAGFP, VSVG-PAGFP, and TfR-PAGFP, respectively. **(f)** σ^{peaks} distribution of an image of PAGFP molecules covalently immobilized on glass coverslip. The σ^{peaks} distributions could be fit to a skewed Gaussian function (red line). The mean (μ) of the fitted Gaussian distribution gives an estimate of the half-width (σ_s) of the Gaussian surface describing the distribution of multiple peaks belonging to a single PAGFP molecule.

Supplementary Note 1. Computation of Correlation Functions

Autocorrelation

Pair autocorrelation function was computed in Matlab using Fast Fourier Transforms as follows:

$$g(\vec{r}) = \frac{FFT^{-1}(|FFT(Im)|^2)}{(\rho^{peaks})^2 N(\vec{r})}$$

Eqn. S1

where FFT^{-1} is an inverse Fast Fourier Transform, Im is the binary PALM image, and $N(r)$ is a normalization accounting for the finite size of the image. To avoid artifactual correlations due to the periodic nature of FFT functions, the image Im is padded with zeros in both directions out to a distance larger than the range of the desired correlation function (800 nm). The normalization factor $N(r)$ is the autocorrelation of a window function W that has the value of 1 inside the measurement area, and is also padded by an equal number of zeros:

$$N(\vec{r}) = FFT^{-1}(|FFT(W)|^2)$$

Eqn. S2

This normalization corrects for the fact that there are fewer possible pairs separated by large distances due to the finite image size. Computed correlation functions were angularly averaged and binned by radius to obtain radial autocorrelation function $g(r)$.

Cross-correlation

Cross-correlation functions between PAGFP and PAmCh labeled fluorescent proteins were computed using FFT as follows:

$$c(\vec{r}) = \text{Real}\left(\frac{FFT^{-1}(FFT(Im^{PAGFP}) \times conj(FFT(Im^{PAmCh})))}{\rho^{PAGFP} \rho^{PAmCh} N(\vec{r})}\right)$$

Eqn. S3

Here $conj()$ indicates a complex conjugate, Im^{PAGFP} and Im^{PAmCh} are the binary PALM images of the PAGFP and PAmCh labeled proteins respectively, ρ^{PAGFP} and ρ^{PAmCh} are the average surface densities of PAGFP and PAmCh peaks respectively, and Real indicates the real part. The normalization factor, $N(r)$, is the correlation of a window function, W , as described above (Eqn. S2). The radial cross-correlation function, $c(r)$ is obtained by angular averaging of the computed cross-correlation functions and binning the values by radius. Experimentally determined cross-correlation functions are expected to be the actual cross-correlation functions between these two proteins convoluted by the average shape of the surface over which the peaks belonging to a single protein are distributed.

Supplementary Note 2. Definition of Mathematical Terms

σ_s	Average localization precision of peaks
$g(r)$	Autocorrelation function
$g(r)^{\text{peaks}}$	Measured autocorrelation function of all peaks in a PALM image
$g(r)^{\text{centroid}}$	Protein autocorrelation at $r = 0$
$g(r)^{\text{protein}}$	Protein autocorrelation at $r > 0$
$g(r)^{\text{PSF}}$	Autocorrelation function of effective point spread function of localization uncertainty
$g(r)^{\text{stoch}}$	Correlation arising from multiple appearance of the same molecule
ξ	Correlation length of clusters
ψ^{cluster}	Increased local density of proteins in a cluster
N^{cluster}	Average number of proteins in a cluster
ρ^{average}	Average density of proteins in a PALM image
ρ^{cluster}	Average density of proteins in a cluster
ρ^{peaks}	Average density of peaks in a PALM image
α	Average number of discrete appearances of a protein due to blinking
$c(r)$	Cross-correlation function